

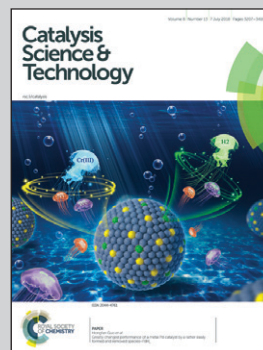


Showcasing collaborative research from Prof. Yoel Sasson group at the Hebrew University, Jerusalem, Israel and Dr. A. P. Singh & Dr. Pradeep Kumar group from CSIR-NCL, Pune, India.

Synthesis of heterogeneous Ru(II)-1,2,3-triazole catalyst supported over SBA-15: application to the hydrogen transfer reaction and unusual highly selective 1,4-disubstituted triazole formation *via* multicomponent click reaction

We demonstrated an efficient protocol for ligand synthesis and covalent tethering to a solid support in a single step using "click chemistry". Exclusively, SBA-15-Tz-Ru(II)TPP screening in multicomponent cycloaddition reaction exhibits remarkable reactivity in water for the regioselective synthesis of 1,4-disubstituted 1,2,3-triazole with excellent yields in one pot.

As featured in:



See A. P. Singh, Pradeep Kumar, Yoel Sasson *et al.*, *Catal. Sci. Technol.*, 2018, 8, 3246.




[rsc.li/catalysis](http://rsc.li/catalysis)

Registered charity number: 207890

Cite this: *Catal. Sci. Technol.*, 2018, 8, 3246

# Synthesis of heterogeneous Ru(II)-1,2,3-triazole catalyst supported over SBA-15: application to the hydrogen transfer reaction and unusual highly selective 1,4-disubstituted triazole formation via multicomponent click reaction†

Priti Sharma,  <sup>‡a</sup> Jayant Rathod, <sup>‡c</sup> A. P. Singh, <sup>\*b</sup> Pradeep Kumar <sup>\*c</sup> and Yoel Sasson <sup>\*a</sup>

In the present study, we demonstrate a simple and efficient method for ligand formation and covalent anchoring to a heterogeneous support via click reaction. The complex tris(triphenylphosphine)ruthenium(II) dichloride [RuCl<sub>2</sub>(PPh<sub>3</sub>)<sub>3</sub>] anchored over the click modified ligand of SBA-15 forms a new highly efficient heterogeneous SBA-15-Tz-Ru(II)TPP catalyst. Solid state <sup>13</sup>C, <sup>29</sup>Si, and <sup>31</sup>P CP-MAS NMR spectra provide evidence for the formation of the heterogeneous catalyst. SBA-15-Tz-Ru(II)TPP catalyst was screened for the multicomponent click cycloaddition reaction in water medium as a green solvent and it exhibited unusual and excellent selectivity for the formation of 1,4-disubstituted triazole product under mild reaction condition. In addition, SBA-15-Tz-Ru(II)TPP catalyst also catalyzed the hydrogen transfer reaction of various carbonyl compounds with excellent catalytic activity to give the corresponding alcohols. The heterogeneous catalyst can be recycled and reused several times (five) without a loss in reactivity.

Received 26th December 2017,  
Accepted 8th April 2018

DOI: 10.1039/c7cy02619f

rsc.li/catalysis

## Introduction

In recent years, the “click chemistry” reaction has grown exceptionally with enhanced attention from worldwide researchers owing to its applications in various fields, such as medicine,<sup>1</sup> materials and polymers.<sup>2</sup> Click chemistry is associated with several advantages, such as a simple and mild reaction procedure, atom efficient, and compatibility with broad range of functional groups.<sup>3</sup> Apart from the extensive applications of click chemistry in various fields, novel ligand design and modification via 1,2,3-triazole have added a new dimension in the area of coordination chemistry. In click chemistry, a high level of selectivity has been demonstrated exclusively for either 1,4 or 1,5-substituted 1,2,3-triazole with excellent yields, with further application as coordination ligands with

various metal complexes.<sup>4</sup> In a remarkable work, Hecht *et al.* utilized click chemistry and its chelating ability to produce a transition metal complex via coordination [clickates based on 2,6-bis(1,2,3-triazol-4-yl)pyridines].<sup>5</sup> In addition, Sarkar and his co-workers designed and synthesized novel ligands via click reaction (1,2,3-triazole) for metal complex coordination and spin crossover complexes.<sup>6</sup> In a book chapter, Crowley *et al.* documented the extension of the applicable light of *click-triazole* in coordination chemistry.<sup>7</sup> With the fact that 1,2,3-triazole shows good capability with metal complexes in coordination chemistry due to its homogeneous nature, it suffers the drawback of recyclability. In our recent work, we have shown that the substituted 1,2,3-triazole can replace the traditional ligand and coordinate with metal complexes via nitrogen-donor ligands in an efficient way.<sup>8</sup> In the same context, we tried to design a new ligand with a covalent attachment to the heterogeneous support in a single step via 1,2,3-triazole formation (click reaction) (Schemes 1 and 2). Further, in the field of heterogeneous catalysis,<sup>9</sup> precisely, mesoporous materials like SBA-15 are preferred candidates for functionalization owing to their high hydrothermal stability, large pore size and thick walls, which can be easily functionalized using the free hydroxyl group of mesoporous SBA-15 (Scheme 2).<sup>10</sup>

In the literature, copper-catalyzed click reactions generally proceed with a two-component reaction system using an

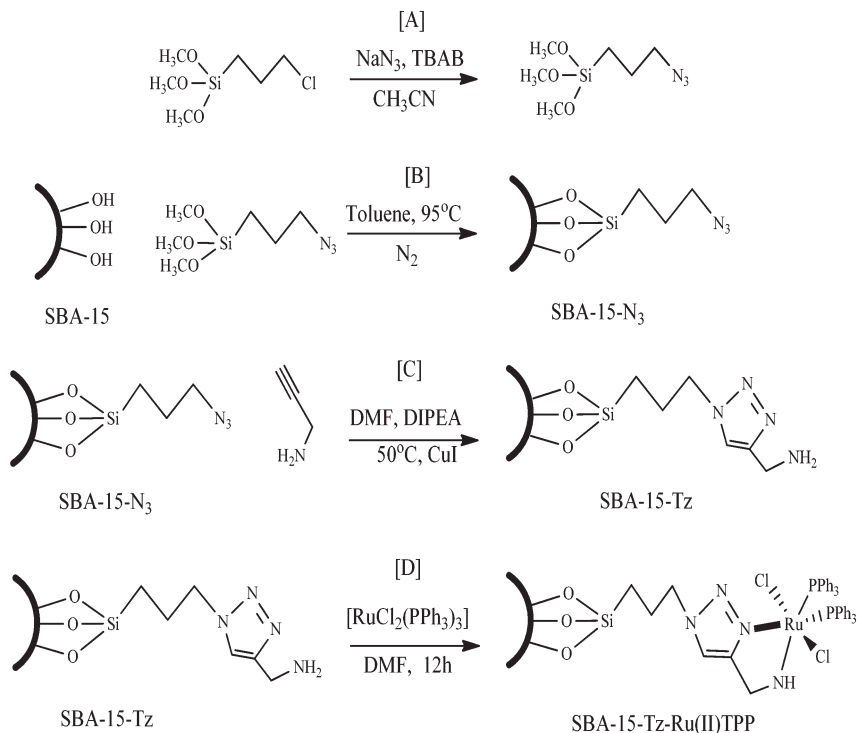
<sup>a</sup> Casali Center of Applied Chemistry, Institute of Chemistry, The Hebrew University of Jerusalem, Jerusalem, Israel. E-mail: ysasson@huji.ac.il

<sup>b</sup> Catalysis Division, CSIR-National Chemical Laboratory, Dr. Homi Bhabha Road, Pune 411008, India. E-mail: ap.singh@ncl.res.in

<sup>c</sup> Division of Organic Chemistry, CSIR-National Chemical Laboratory, Dr. Homi Bhabha Road, Pune-411008, India. E-mail: pk.tripathi@ncl.res.in

† Electronic supplementary information (ESI) available: <sup>31</sup>P NMR of catalyst SEM-EDX analysis, TEM images, TEM-EDX, XPS result, P XPS, <sup>1</sup>H NMR of Intermediate 4-phenyl-1H-1,2,3-triazole, ICP, HR-XPS, analytical data of multi component click cycloaddition products. See DOI: 10.1039/c7cy02619f

‡ Equal contribution.



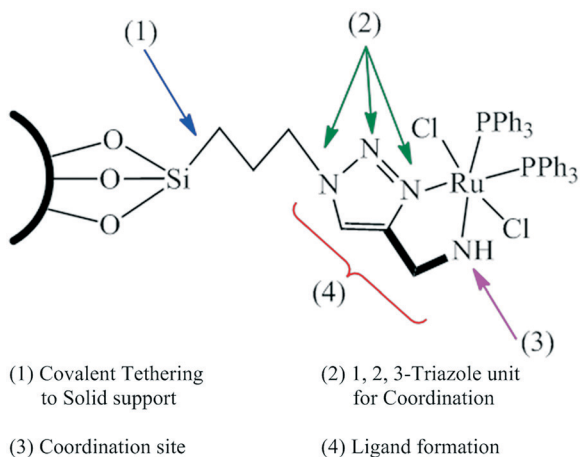
**Scheme 1** Schematic diagram of (A) 3-azidopropyltrimethoxysilane synthesis, (B) azide-organofunctionalization over SBA-15, (C) SBA-15 ligand fabrication via 2-propargylamine, and (D)  $[\text{RuCl}_2(\text{PPh}_3)_3]$  complex anchoring over SBA-15-Tz.

organic azide.<sup>11</sup> However, organic azides, the key component of the click reaction, are prone to explode and are highly hazardous in the processes of purification and isolation.<sup>12</sup> Some reports are available by following *in situ* azide synthesis, but they face the drawbacks of tedious procedures coupled with high temperatures and long reaction times, which might lead to side product formation (homo coupling) and 1,5-disubstituted 1,2,3-triazole.<sup>13</sup>

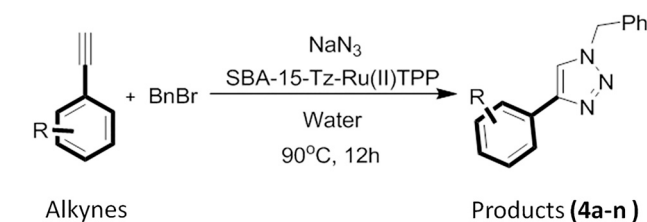
Recently, apart from copper, many other metals,<sup>14</sup> such as ruthenium<sup>15</sup> complexes, have been reported to catalyze the cycloaddition of terminal acetylenes and azides selectively to

give 1,5 or 1,4-disubstituted triazoles.<sup>16</sup> In a remarkable piece of work, Liu and co-workers reported a catalyst-dependent regioselective click reaction with the homogeneous cyclopentadienyl ligand free Ru-catalyst, for the selective formation of 1,4-disubstituted 1,2,3-triazole.<sup>17</sup> In the same context, in the multicomponent protocol presented here, selective 1,4-disubstituted 1,2,3-triazole regioselective product is achieved by using SBA-15-Tz-Ru(II)TPP heterogeneous catalyst. However, the reaction sequence starts with the Ru-catalyzed cycloaddition of azide and alkyne to give the intermediate 4-phenyl-1H-1,2,3-triazole followed by a sequential *in situ* substitution reaction with benzyl bromide to give the 1,4-disubstituted 1,2,3-triazole compounds by homogeneous  $\text{RuCl}_2(\text{PPh}_3)_3$  complex and heterogeneous SBA-15-Tz-Ru(II)TPP catalyst (Schemes 3 and 5a-c).

Catalytic hydrogen transfer (CTH) reactions were developed as an alternative to the traditional catalytic hydrogenation processes and to avoid the use of hydrogen gas under pressure.<sup>18,19</sup> The hydrogen transfer reaction has been



**Scheme 2** Schematic representation of click chemistry usage in ligand formation and covalent anchoring in an elementary step.



**Scheme 3** Multicomponent click cycloaddition model reaction.

performed employing catalysts such as homogenous catalysts,<sup>20</sup> metal alloys,<sup>21</sup> metal oxides<sup>22</sup> and organometallic complexes<sup>23</sup> on various solid supports.<sup>24</sup> However a broad range of hydrogen transfer reactions are covered by various ruthenium catalysts.<sup>18d,25</sup> Unfortunately, the reported processes generally progress in harsh reaction conditions and most of them are not recyclable.<sup>26</sup> The best use of homogeneous catalysts is through heterogenization over a solid support.

Herein, we report a new heterogeneous catalyst complex,  $[\text{RuCl}_2(\text{PPh}_3)_3]$ , over 1,4-substituted 1,2,3-triazole liganded SBA-15 (click modified) and the screening of its catalytic properties in multicomponent click cycloaddition and hydrogen transfer reaction.

## Results and discussion

The synthesis strategy employed to fabricate SBA-15-Tz-Ru(*n*)TPP heterogeneous catalysts is shown in Scheme 1. As per Scheme 1, the free hydroxyl group of the mesoporous SBA-15 heterogeneous support is first covalently anchored by azido linker group (3-Az-PTMS), and then modified to a triazole ligand *via* click reaction by propargylamine. Further, the procedure involves stirring and refluxing a mixture of click-functionalized SBA-15-Tz with a solution of  $[\text{RuCl}_2(\text{PPh}_3)_3]$  in DMF for 12 h under argon atmosphere (Scheme 1).

The synthesized catalysts were characterized by different physicochemical characterization techniques and the results are discussed here in detail. The XRD patterns of SBA-15 (a), SBA-15-N<sub>3</sub> (b), SBA-15-Tz (c) and SBA-15-Tz-Ru(*n*)TPP (d) are presented in Fig. 1. The observed X-ray diffraction pattern demonstrates the characteristic highly ordered hexagonal mesoporous silica framework of the synthesized click-modified materials (Fig. 1).<sup>27</sup> The characteristic hexagonal phase (*p6mm*) of SBA-15 shows three reflection planes: an intense peak at (100) and peaks with low intensity at (110) and (200) are visible in all modified SBA-15 materials at  $2\theta = 0.949^\circ$ ,  $1.565^\circ$  and  $1.799^\circ$ , respectively. The observed results support a high degree of

orderedness of the two dimensional (2D) hexagonal phase (Fig. 1a).<sup>28</sup> The peak intensities of the reflections (100) in SBA-15-N<sub>3</sub>, SBA-15-Tz and SBA-15-Tz-Ru(*n*)TPP are in decreasing order from calcined SBA-15 to modified SBA-15 material moderately in Fig. 1(a-d), owing to surface modification and anchored organometallic complex, respectively, by using the free clickable surface of SBA-15 (Fig. 1a-d).<sup>29</sup>

FTIR spectra indicate the presence of surface silanols, hydroxyl group, anchored complex, and  $\text{RuCl}_2(\text{PPh}_3)_3$  in (a) calcined SBA-15, (b) SBA-15-N<sub>3</sub>, (c) SBA-15-Tz, (d) SBA-15-Tz-Ru(*n*)TPP, (e)  $\text{RuCl}_2(\text{PPh}_3)_3$ , and (f) 3-Az-PTMS materials in Fig. 2. The strong visible bands in the range of  $807\text{--}770\text{ cm}^{-1}$  and  $1038\text{--}1090\text{ cm}^{-1}$  are attributable to the symmetric and asymmetric stretching vibrations of the Si-O-Si bonds in the SBA-15 and modified SBA-15 materials, respectively (Fig. 2a-d).<sup>8,27,29</sup> Further, a strong band is observed in the mid-infrared region at  $906\text{ cm}^{-1}$ , attributed to the Si-OH vibrations (Fig. 2a-d). The FT-IR spectra of SBA-15-N<sub>3</sub>, SBA-15-Tz and SBA-15-Tz-Ru(*n*)TPP materials exhibit two bands at  $2990\text{ cm}^{-1}$  and  $2891\text{ cm}^{-1}$ , which are from the asymmetric and symmetric vibrations of the -CH<sub>2</sub> groups of the linker propyl chain (3-azidopropyltrimethoxy silane) (Fig. 2b-d), respectively. Furthermore, SBA-15-N<sub>3</sub> shows a sharp absorbance at  $2104\text{ cm}^{-1}$ , the characteristic stretching vibration of organic azide (-N<sub>3</sub>). The presence of a similar absorption band visible in the pure homogeneous 3-azidopropyltrimethoxysilane linkers ( $2104\text{ cm}^{-1}$ ) proves successful anchoring of the linker to calcined SBA-15 (Fig. 2b and f).<sup>30</sup> Further, the complete consumption of the above-mentioned (-N<sub>3</sub>,  $2104\text{ cm}^{-1}$ ) characteristic peak in SBA-15-Tz material demonstrates that the 3-azidopropyl tethering agent successfully reacted with propargylamine *via* click reaction (Fig. 2c). Strong characteristic vibrations of PPh<sub>3</sub> (aromatic region) complex in FT-IR are found at  $683$ ,  $700$ ,  $1076$ ,  $1437$ ,  $1481$  and  $3050\text{ cm}^{-1}$  in the homogeneous catalyst, whereas with less intensity the same vibrations are visible in the heterogeneous catalyst SBA-15-Tz-Ru(*n*)TPP, supporting the fact that the PPh<sub>3</sub> group may leave

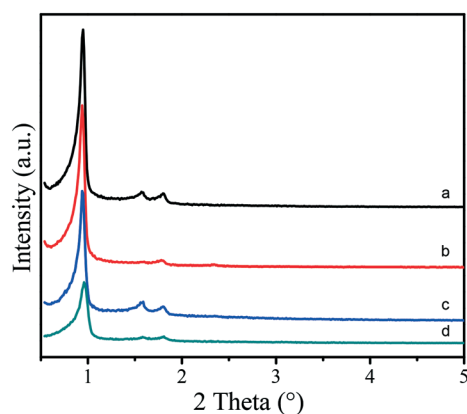


Fig. 1 Small angle XRD patterns of (a) SBA-15, (b) SBA-15-N<sub>3</sub>, (c) SBA-15-Tz, and (d) SBA-15-Tz-Ru(*n*)TPP.

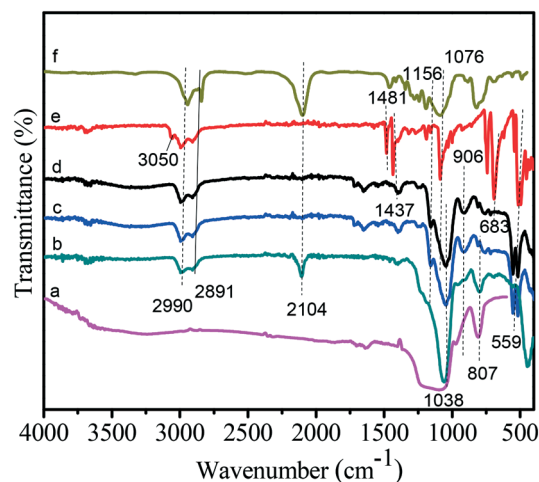


Fig. 2 FT-IR spectra of (a) calcined SBA-15, (b) SBA-15-N<sub>3</sub>, (c) SBA-15-Tz, (d) SBA-15-Tz-Ru(*n*)TPP, (e)  $\text{RuCl}_2(\text{PPh}_3)_3$ , and (f) 3-Az-PTMS.

the complex after anchoring (due to *trans* effect) (Fig. 2e and d).<sup>31</sup> The spectra of the heterogenized complex SBA-15-Tz-Ru(II)TPP catalyst display characteristic peaks of the neat catalyst, indicating the structural retention of the [RuCl<sub>2</sub>(PPh<sub>3</sub>)<sub>3</sub>] complex after immobilization.

The <sup>13</sup>C solid state CP MAS NMR spectra of (a) SBA-15-N<sub>3</sub> and (b) SBA-15-Tz-Ru(II)TPP are depicted in Fig. 3. The peaks at 10, 23 and 54 ppm are assigned to the carbon atoms of the linker propyl chain in the azido (SBA-15-N<sub>3</sub>) group, indicating covalent azido functionalization of SBA-15 (Fig. 3a). The appearance of additional intense peaks precisely in the aromatic region of the PPh<sub>3</sub> group from 117 to 138 ppm (consisting 127, 143, 144, 146) clearly demonstrates the functionalization of the Ru(II)TPP complex over the clickable SBA-15 support (Fig. 3b).<sup>8,30a,32</sup> These NMR results demonstrate the successful immobilization of the [RuCl<sub>2</sub>(PPh<sub>3</sub>)<sub>3</sub>] complex on the clickable surface of the SBA-15 support.

The functionalization of free hydroxyl groups of SBA-15 with an organic moiety could be confirmed by <sup>29</sup>Si CP MAS NMR spectroscopy. Fig. 4(A and B) exhibits the <sup>29</sup>Si CP MAS NMR spectra of calcined SBA-15 and SBA-15-Tz-Ru(II)TPP catalyst. The spectrum in Fig. 4A exhibits broad resonance peaks from -90 to -120 ppm, which are indicative of a range of Si-O-Si bond, while the bands centered at -93 ppm, -102 ppm and -111 ppm are assigned to the Q<sup>2</sup> [(SiO)<sub>2</sub>Si(OH)<sub>2</sub>], Q<sup>3</sup> [(SiO)<sub>3</sub>Si(OH)] and Q<sup>4</sup> [(SiO)<sub>4</sub>Si] sites of the framework of SBA-15, respectively (Fig. 4B). In general, the Q<sup>3</sup> sites are considered to be loaded with Si-OH groups. The Q<sup>2</sup> sites are frequently attainable for possible anchoring with organic complexes. The <sup>29</sup>Si CP MAS NMR spectrum of SBA-15-Tz-Ru(II)TPP shows two peaks at -67 ppm and -60 ppm, which are assigned to T<sup>3</sup> [Si(OSi)<sub>3</sub>] and T<sup>2</sup> [Si(OH)R(OSi)<sub>2</sub>], respectively (Fig. 4B).<sup>27a,29,30</sup> The presence of a sharp T<sup>3</sup> peak indicates the covalent anchoring of 3-azidopropyltrimethoxy silane over the clickable mesoporous SBA-15 surface for further anchoring of the complex (Fig. 4B) (ESI,† Fig. S7).

The <sup>31</sup>P CP MAS NMR spectrum of heterogeneous catalyst SBA-15-Tz-Ru(II)TPP exhibits two <sup>31</sup>P signals at *d* = 34 and 50 ppm (Fig. S1†). After interacting with the click modified SBA-

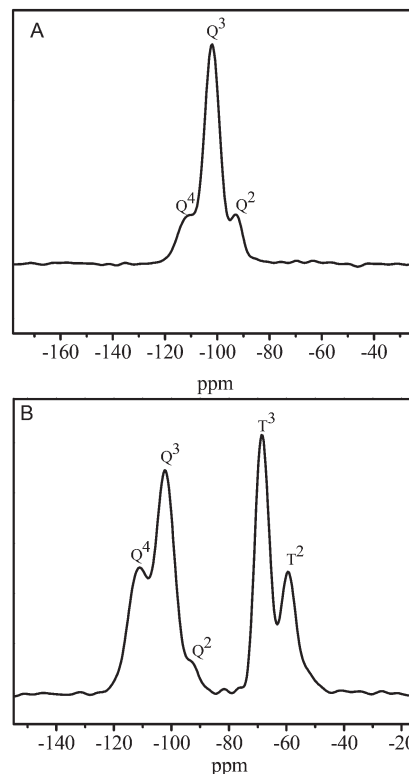


Fig. 4 <sup>29</sup>Si CP-MAS NMR of (A) calcined SBA-15 and (B) SBA-15-Tz-Ru(II)TPP.

15 triazole ligand, one equatorial PPh<sub>3</sub> group leaves from the RuCl<sub>2</sub>(PPh<sub>3</sub>)<sub>3</sub> homogeneous complex system (owing to the strong *trans* effect of another PPh<sub>3</sub> group, two non-equivalent phosphorus environments).<sup>31,33</sup> The spectrum contains two signals (*d* = 34, 50 ppm) that are merged into one intense peak, indicating the presence of two non-equivalent phosphorus atoms in the synthesized catalyst SBA-15-Tz-Ru(II)TPP (Fig. S1†).

The observed nitrogen adsorption-desorption results of SBA-15 and SBA-15-Tz-Ru(II)TPP with the corresponding pore size distribution curves are plotted in Fig. 5 and the details

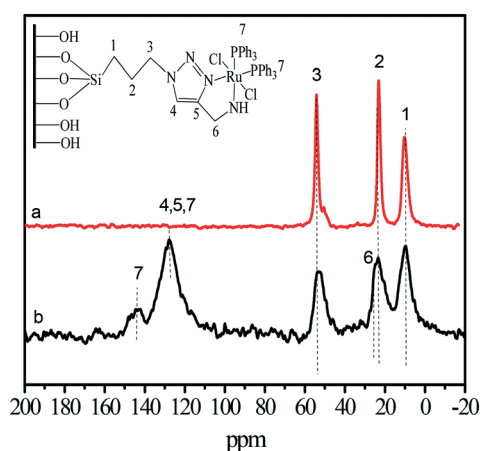


Fig. 3 <sup>13</sup>C CP-MAS NMR of (a) SBA-15-N<sub>3</sub> and (b) SBA-15-Tz-Ru(II)TPP.

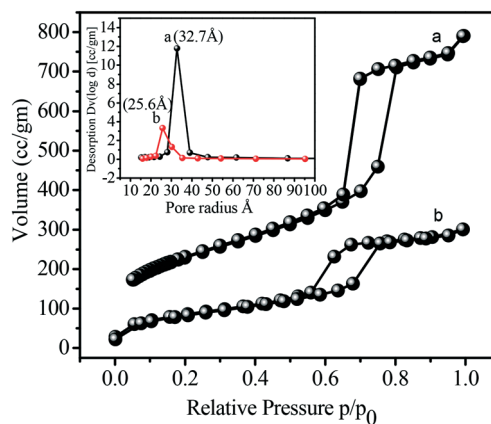


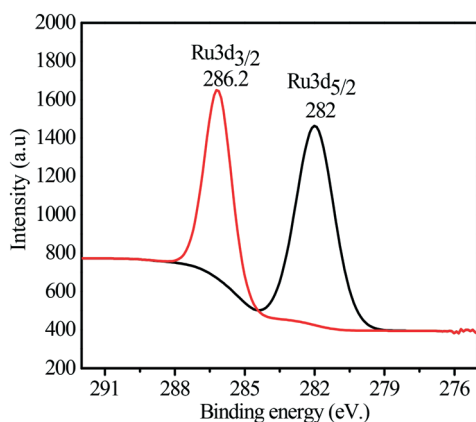
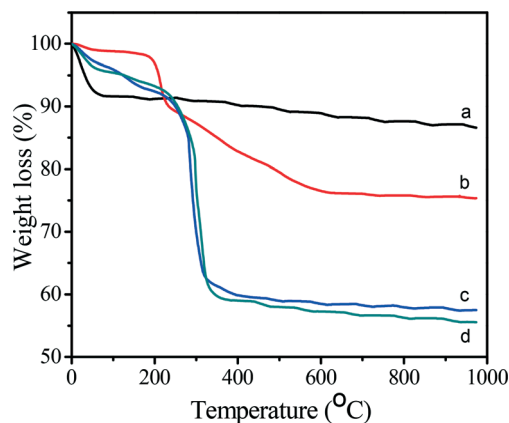
Fig. 5 N<sub>2</sub> adsorption-desorption isotherm and pore size distribution (inset) of (a) calcined SBA-15 and (b) catalyst SBA-15-Tz-Ru(II)TPP.

**Table 1** Textural properties of SBA-15 and catalyst SBA-15-Tz-Ru(II)TPP

	BET surface area ( $\text{m}^2 \text{g}^{-1}$ )	Average pore radius ( $\text{\AA}$ )	Pore volume ( $V_p$ , $\text{cm}^3 \text{g}^{-1}$ )
SBA-15	830.7	32.7	1.13
SBA-15-Tz-Ru(II)TPP	314.6	25.696	0.425

are summarized in Table 1. The surface area, average pore diameter and pore volume observed for SBA-15 and SBA-15-Tz-Ru(II)TPP catalyst are summarized in Table 1. Both synthesized materials SBA-15 and SBA-15-Tz-Ru(II)TPP exhibit type IV adsorption isotherms with a hysteresis characteristic for mesoporous materials with uniform size and completely reversible nature, with a capillary condensation step at  $P/P_0 = 0.3\text{--}0.4$  (as per IUPAC classification). The total surface area, average pore radius and pore volume for SBA-15 and SBA-15-Tz-Ru(II)TPP were observed to be  $830 \text{ m}^2 \text{g}^{-1}$ ,  $32.7 \text{ \AA}$ , and  $1.13 \text{ cm}^3 \text{g}^{-1}$ , and  $314 \text{ m}^2 \text{g}^{-1}$ ,  $25.7 \text{ \AA}$ , and  $0.425 \text{ cm}^3 \text{g}^{-1}$ , respectively. The noticeable change (decrease) in the total mesoporous surface area (62%), pore radius (21%) and pore volume (53%) after tris(triphenylphosphine)ruthenium(II) dichloride  $[\text{RuCl}_2(\text{PPh}_3)_3]$  immobilization over click modified SBA-15 is indicative of the successful immobilization of the complex over the mesoporous SBA-15 (Table 1) and consistent with the XRD and XPS results (Fig. 1, 5, and 6).

The XPS spectrum of SBA-15-Tz-Ru(II)TPP is displayed in Fig. 6. The accuracy of the observed binding energy (B.E.) is  $\pm 0.3 \text{ eV}$ . The Ru3d core level XPS spectrum shows two (B.E.) peaks centered at 282 eV and 286 eV, respectively. The first peak (282 eV) is well resolved and can be assigned to the BE of Ru3d<sub>5/2</sub>. As the second peak (286 eV) is associated with the contribution Ru3d<sub>3/2</sub>, the peak at 286 eV is deconvoluted and can be assigned to the existence of Ru in the +2 oxidation state in catalyst SBA-15-Tz-Ru(II)TPP (Fig. 6).<sup>34</sup> The P XPS analysis values for the 2p<sub>3/2</sub> and 2p<sub>1/2</sub> core levels are distinguished at 131.3 and 132.1, respectively (Fig. S5†). The XPS value for phosphorous (P) in SBA-15-Tz-Ru(II)TPP is in good agreement with the literature value and confirms the  $[\text{RuCl}_2(\text{PPh}_3)_3]$  complex is retained when anchored over the organomodified support SBA-15 (Fig. S6).<sup>31a</sup> The presence of

**Fig. 6** Ru XPS spectrum of SBA-15-Tz-Ru(II)TPP.**Fig. 7** TGA analysis of: (a) Calcined SBA-15, (b) SBA-15-N<sub>3</sub>, (c) SBA-15-Tz, and (d) SBA-15-Tz-Ru(II)TPP.

Ru, P, and Cl elements in SBA-15-Tz-Ru(II)TPP is confirmed by complete HR-XPS spectrum (ESI† Fig. S8).

The thermal behavior of all the synthesized materials (A) SBA-15, (B) SBA-15-N<sub>3</sub>, (C) SBA-15-Tz, and (D) SBA-15-Tz-Ru(II)TPP was studied by thermogravimetric analysis (TGA) in air atmosphere from room temperature up to 1000 °C with an increment of  $10 \text{ }^\circ\text{C min}^{-1}$  (Fig. 7). The TGA plots of all click-modified SBA-15 samples show nearly 6% weight loss below 120 °C owing to the desorption of adsorbed water molecules (Fig. 7a–d). In the shown TGA plot, almost no weight loss was observed for the calcined SBA-15 material between 120 °C and 200 °C, indicating the complete discharge of surfactant from SBA-15 (Fig. 7a). The TGA results of the SBA-15-N<sub>3</sub> material show weight loss in two steps. In the first step, a weight loss between 70 °C and 140 °C corresponds to the loss of water (adsorbed moisture). In the second step, a weight loss was observed in the range of 255–365 °C, temperature regions attributed to 3-Az-PTMS (Fig. 7b). The TGA plot of SBA-15-N<sub>3</sub> quantitatively shows the  $\sim 11.25\%$  weight loss, which is greater than the calcined SBA-15, strongly supporting the on-track anchoring of the 3-Az-PTMS over SBA-15 (Fig. 7a and b). In the case of the click-modified triazole complex SBA-15-Tz, one extra weight loss step in the range of 250 to 350 °C was observed along with the existing weight losses seen for SBA-15-N<sub>3</sub> (Fig. 7b and c). A categorical comparison of heterogenized SBA-15-Tz-Ru(II)TPP and functionalized SBA-15-Tz in terms of weight loss shows  $\sim 2$  weight% loading of the complex material and the results are in good agreement with those obtained from XPS and ICP-OES (Fig. 7a–d, Fig. S5 and S9†).

The SEM images of (A) SBA-15 and (B) SBA-15-Tz-Ru(II)TPP are shown in Fig. 8. The morphology of SBA-15-Tz-Ru(II)TPP was matched with the host mesoporous material SBA-15 after the anchoring of the  $[\text{RuCl}_2(\text{PPh}_3)_3]$  complex on the azido-functionalized SBA-15.<sup>27a,30a</sup> The calcined SBA-15 shows a cylindrical rod-like structure with wormlike morphology in the SEM images. Further, SBA-15-Tz-Ru(II)TPP was demonstrated to be a similar molecular based material; the large molecular system changes to be closely compacted together with respect to the SBA-15 after the  $[\text{RuCl}_2(\text{PPh}_3)_3]$  complex is immobilized

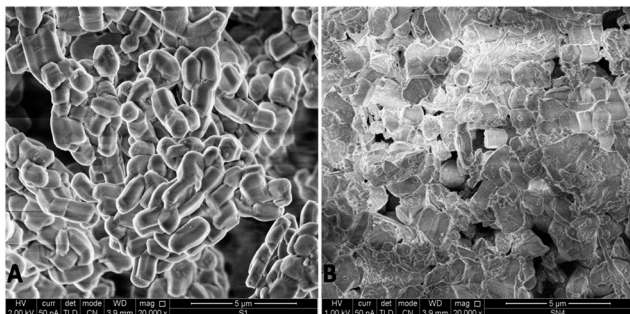


Fig. 8 SEM images of (A) calcined SBA-15 and (B) SBA-15-Tz-Ru(II)TPP.

over the clickable mesoporous surface (Fig. 8A and B). Moreover, the EDX patterns of SBA-15 and SBA-15-Tz-Ru(II)TPP indicate the presence of ruthenium in the synthesized heterogeneous catalyst SBA-15-Tz-Ru(II)TPP (Fig. S2†).

The TEM images of the SBA-15 and SBA-15-Tz-Ru(II)TPP provide structural evidence that the material is organized into ordered arrays of two-dimensional hexagonal mesopores and the parallel channel structure with thick walls of the mesoporous materials can be clearly visualized with different magnifications (Fig. 9A and B, ESI† S3). However, after the anchoring of the  $[\text{RuCl}_2(\text{PPh}_3)_3]$  complex over the clickable mesoporous channels of SBA-15, the images show darker contrast *meso* parallel channels, in comparison to the SBA-15 surface, corresponding to the proper anchoring of  $[\text{RuCl}_2(\text{PPh}_3)_3]$  complex over the clickable surface of the SBA-15 (Fig. 9A and B).<sup>27</sup> EDX obtained from TEM analysis evidently confirms the presence of elemental ruthenium and phosphorous in the heterogeneous catalyst SBA-15-Tz-Ru(II)TPP (Fig. S4†).

### Catalytic activity

**Multicomponent click reaction.** After thorough characterization, we proceeded further in screening of multicomponent click cycloaddition of the alkyne, azide and alkyl halide (Scheme 3). This represents a powerful method for 1,4-disubstituted 1,2,3-triazole formation compared to the traditional two component click reaction. Extensive research has been done on multicomponent reactions, but only a few of

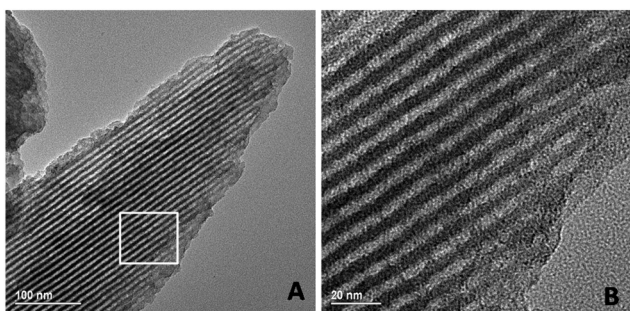


Fig. 9 TEM images of SBA-15-Tz-Ru(II)TPP at different magnifications: (A) 100 nm and (B) 20 nm.

them are recyclable and they need additives for enforced recycling, *e.g.* supported copper catalyst.<sup>35</sup> However, these catalytic system suffers from drawbacks, including the use of additives, such as sodium ascorbate, and organic solvents, such as dioxane or acetonitrile, for the reactions.<sup>36</sup> We began with optimizing the multicomponent click reaction of phenyl acetylene, sodium azide and benzyl bromide using homogeneous Ru catalyst with respect to solvent and ligands and compared the results with our synthesized heterogeneous Ru catalyst in terms of the regioselectivity of the triazole formation (Table 2). As per literature precedence, the click reaction using Ru as the catalyst gives the 1,5-disubstituted triazole heterocycles. When the Cu salt is used as the catalyst, it shows different selectivity and provides the 1,4-disubstituted triazoles. There are only two reports for the Ru catalyzed click reaction, which show contradictory results to the usual outcome for reaction with certain limitations. Considering this, we hypothesized the multi-component click reaction of alkyne, sodium azide and benzyl bromide.

In order to optimize the reaction conditions, phenyl acetylene, sodium azide and benzyl bromide were selected as model substrates and screened with various Ru catalysts for the click reaction. We began with  $\text{RuCl}_3$  as the catalyst and  $\text{PPh}_3$  as the ligand using DMF as the solvent at 90 °C; the reaction ended up with very poor yields and reverse selectivity (*i.e.*, 1,4 substituted triazole) (Table 2, entry 1). To further optimize the reaction conditions, various solvents, such as DMSO, dioxane, and toluene, were tested but unfortunately there was little improvement with a maximum yield of 26% (Table 2, entries 2–4). To our delight, when the reaction was performed using water as the solvent, the yield was increased to 48% with reverse selectivity. To optimize the yield, the reaction was performed with different ligands, such as DMAP and 2-amino-6-picoline, but this ended up lowering the yield of the product (Table 2, entries 6 and 7). When the Ru catalyst was changed to  $[\text{Ru}(p\text{-cym})\text{Cl}]_2$ , no improvement in the yield was observed, we then considered the reaction in homogeneous conditions, switching over to heterogeneous conditions from the homogeneous. Accordingly, when the reaction performed with organosilica-supported Ru catalyst SBA-15-Tz-

Table 2 Optimization of multicomponent cycloaddition reaction in homogeneous and heterogeneous medium

S. No.	Catalyst	Ligand	Solvent	Yield (%)
1.	$\text{RuCl}_3$	$\text{PPh}_3$	DMF	6
2.	$\text{RuCl}_3$	$\text{PPh}_3$	DMSO	24
3.	$\text{RuCl}_3$	$\text{PPh}_3$	Dioxane	26
4.	$\text{RuCl}_3$	$\text{PPh}_3$	Toluene	5
5.	$\text{RuCl}_3$	$\text{PPh}_3$	Water	48
6.	$\text{RuCl}_3$	DMAP	Water	32
7.	$\text{RuCl}_3$	2-Amino-6-picoline	Water	10
8.	$[\text{Ru}(p\text{-cym})\text{Cl}]_2$	—	Water	26
9.	SBA-15-Tz-Ru(II)TPP	—	Water	88

Reaction conditions: phenyl acetylene (1 mmol), benzyl bromide (1.2 mmol), sodium azide (1.2 mmol), catalyst (ruthenium 0.445 mol%) and solvent (3 mL).

**Table 3** Solvent optimization for multicomponent cycloaddition reaction

Entry	Solvent	Time (h)	Temperature (°C)	Yield (%)
1.	DMSO	24	RT	00
2.	DMSO	12	90	46
3.	DMF	12	90	63
4.	<i>t</i> -BuOH	12	90	35
5.	EtOH	24	90	50
6.	H <sub>2</sub> O	12	90	88
7.	H <sub>2</sub> O	24	RT	00
8.	THF	12	90	20

Reaction conditions: phenyl acetylene (1 mmol), benzyl bromide (1.2 mmol), sodium azide (1.2 mmol), SBA-15-Tz-Ru(II)TPP catalyst (15 mg, ruthenium metal 0.445 mol%) and solvent (3 mL).

Ru(II)TPP in water as the solvent, the reaction proceeded very smoothly with excellent yield of the desired product and with reverse selectivity (88%) (Table 2, entry 9).

We further proceeded to optimize the reaction conditions with the heterogeneous catalyst to establish a protocol in water as a green solvent. A few catalytic systems are active in aqueous solution, such as CuSO<sub>4</sub>/copper ion complex,<sup>37</sup> but with a high concentration of copper complex. We optimized the multicomponent click reaction with respect to solvent and temperature, and the results are summarized in Tables 3 and 4.

A variety of solvents, such as DMSO, DMF, EtOH, *t*-BuOH, THF and water, were screened in the presence of SBA-15-Tz-Ru(II)TPP catalyst at 90 °C in a model reaction of the multicomponent click cycloaddition between phenyl acetylene (1 mmol), benzyl bromide (1.2 mmol) and sodium azide (1.2 mmol) (Table 3). Solvents like DMSO, DMF, EtOH, *t*-BuOH and THF were not able to give a significant yield (20–63%) even after 24 h reaction time period (Table 3, entries 1–5 and 8). In addition, the reaction was also carried out at room temperature using SBA-15-Tz-Ru(II)TPP catalyst in the presence of water and DMSO solvent under similar reaction conditions, but no reaction progress was observed, even after 24 h of reaction (Table 3, entries 1 and 7). The green solvent water was found to be the most suitable under the optimized reaction conditions (Table 3, entry 9). From the obtained results of the solvent optimization for the conversion of phenylacetylene, the reactivity order of solvents emerged as follows: water (88%) > DMF (63%) > EtOH (50%) > DMSO (46%) > *t*-BuOH (35%) > THF (20%).

Lower temperature does not favor the formation of the product (1,4-disubstituted 1,2,3-triazole). However, the yield of the triazole increased sharply up to 88% with an increase in the reaction temperature to 90 °C for 12 h under optimized reaction conditions. It is noteworthy that the optimum reaction temperature concerning conversion towards the triazole product, under the present reaction conditions, was found to be 90 °C. To establish the proficiency in catalytic activity of synthesized heterogeneous SBA-15-Tz-Ru(II)TPP catalyst under optimized reaction conditions, a wide range of nonsubstituted and substituted phenyl acetylenes were allowed to react with benzyl halides and sodium azide to produce the corresponding triazole, in good to excellent yields

(Table 4). The mono-substituted phenyl acetylenes afforded the triazole product in 88% yield (Table 4, entry 1). It is evident that the electron withdrawing or electron donating groups (EWG and EDG) attached to the phenyl acetylenes do not affect the rate of reaction very much (Table 4, entries 2–10). The methyl (–CH<sub>3</sub>), nitro (–NO<sub>2</sub>), –CN and –COMe substituted phenyl acetylenes reacted smoothly and provided excellent yield of the respective triazoles (Table 4 entries 2, 5, 3, 6). Similarly, the reaction with alkoxy-substituted phenyl acetylene also furnished the corresponding product in good to excellent yield (Table 4 entries 4, 7–9). Interestingly, the bulky aromatic acetylenes also afforded the corresponding product in excellent yield (~89%) (Table 4, entry 10) (ESI† S10 and S11).

Although; the exact mechanism is not clearly understood at this point, to support the regioselective formation of the 1,4-disubstituted 1,2,3-triazole product, a few controlled experiments were performed. In the present study, Ru-catalyzed multicomponent reaction gives exclusively the regioselective 1,4-disubstituted triazole compounds.<sup>38</sup> As our proposed method is multicomponent, the opposite regioselectivity can be achieved; the reaction sequence first follows the Ru-catalyzed cycloaddition of azide and alkyne to give the intermediate 4-phenyl-1*H*-1,2,3-triazole followed by sequential *in situ* substitution reaction with benzyl bromide to give the reported 1,4-disubstituted 1,2,3-triazole compounds (Scheme 5a). To prove our hypothesis, first the reaction was carried out without benzyl bromide, which was completed within six hours furnishing the 4-phenyl-1*H*-1,2,3-triazole in excellent yield (83%) under the optimized reaction conditions (NMR data are in good agreement with the literature report) (Scheme 5b) (see ESI† for NMR detail, S11). The isolated intermediate when subjected to substitution reaction with benzyl bromide under the similar reaction conditions afforded the expected 1,4-disubstituted 1,2,3-triazole product (Scheme 5c). The same product was obtained even employing the homogeneous catalyst tris-(triphenylphosphine)ruthenium(II) dichloride [RuCl<sub>2</sub>(PPh<sub>3</sub>)<sub>3</sub>]. The plausible mechanism for the regioselective formation of 1,4-disubstituted triazole is given in Fig. 10.

### Hydrogen transfer reaction

Generally, the classical hydrogen transfer reaction needs a dry organic solvent, an inert atmosphere, prolonged reaction time period and homogeneous catalysts.<sup>11a,39</sup> Backvall *et al.* reported appreciable activity of various homogeneous ruthenium-catalyzed hydrogen transfer reactions of different ketones.<sup>40</sup> In addition, a few groups have demonstrated the potential of other metal complexes in homogeneous systems for hydrogen transfer reactions. However, these catalytic systems face the drawbacks of tedious synthesis procedure, low TON, and no recycling of expensive catalysts.<sup>41</sup> Conversely, the present developed protocol has the benefits of a minimal amount of catalyst combined with the reuse and recycling of the catalyst with high TON under ambient catalytic reaction conditions.



**Table 4** Multicomponent click cycloaddition using SBA-15-Tz-Ru(II)TPP

Alkyne + BnBr  $\xrightarrow[90^\circ\text{C}, 12\text{h Water}]{\text{NaN}_3, \text{SBA-15-Tz-Ru(II)TPP}}$  Product 4(a-n)

S. No.	Alkynes	Product	Yield <sup>a</sup> (%)	Entry
1.			88	4a
2.			86	4b
3.			92	4c
4.			78	4d
5.			82	4e
6.			77	4f
7.			86	4g
8.			70	4h
9.			76	4i
10.			89	4j
11.			87 <sup>b</sup>	4k
12.			85	4l
13.			73 <sup>c</sup>	4m

Table 4 (continued)

S. No.	Alkynes	Product	Yield <sup>a</sup> (%)	Entry
14.			76 <sup>d</sup>	4n

Reaction conditions: phenyl acetylene (1 mmol), benzyl bromide (1.2 mmol), sodium azide (1.2 mmol), catalyst SBA-15-Tz-Ru(II)TPP (15 mg, ruthenium metal 0.445 mol%) and solvent (3 mL), time period 12 h. <sup>a</sup> Isolated yields. <sup>b</sup> PMB-Cl was used in place of BnBr. <sup>c</sup> 1-Decyne as alkyne. <sup>d</sup> 1-Bromobutane was used in place of BnBr.

The synthesized heterogeneous SBA-15-Tz-Ru(II)TPP catalyst was investigated for hydrogen transfer reaction using cyclohexanone as a model substrate. Under the optimized reaction conditions, the heterogeneous catalyst SBA-15-Tz-Ru(II)TPP (30 mg), isopropanol (10 mL), 2-cyclohexanone (2 mmol) and NaOH (0.5 mmol) were stirred at 80 °C (Scheme 4). The progress of the reaction was monitored by GC. After the completion of the reaction, the usual workup gave the expected product in excellent yields.

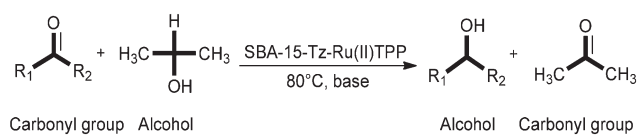
To demonstrate the catalytic strength of SBA-15-Tz-Ru(II)TPP, a blank reaction was carried out without SBA-15-Tz-Ru(II)TPP catalyst and no product was detected by GC even after 24 h using isopropanol and cyclohexanone as the standard substrates under the optimized reaction conditions.

In order to further optimise the reaction conditions, various bases, such as NEt<sub>3</sub>, NaHCO<sub>3</sub>, KOH, NaOH and K<sub>2</sub>CO<sub>3</sub>, were screened for the model reaction [substrates: isopropanol (10 mL) and cyclohexanone (2 mmol)]. The order of reactivity for the transfer hydrogenation reaction of cyclohexanone in the presence of various bases could be arranged as follows: NaOH (100%) > KOH (98%) > K<sub>2</sub>CO<sub>3</sub> (50%) > NaHCO<sub>3</sub> (40%) ≫ NEt<sub>3</sub> (10%). NaOH was found to be the most suitable base for the reaction (Table 5).

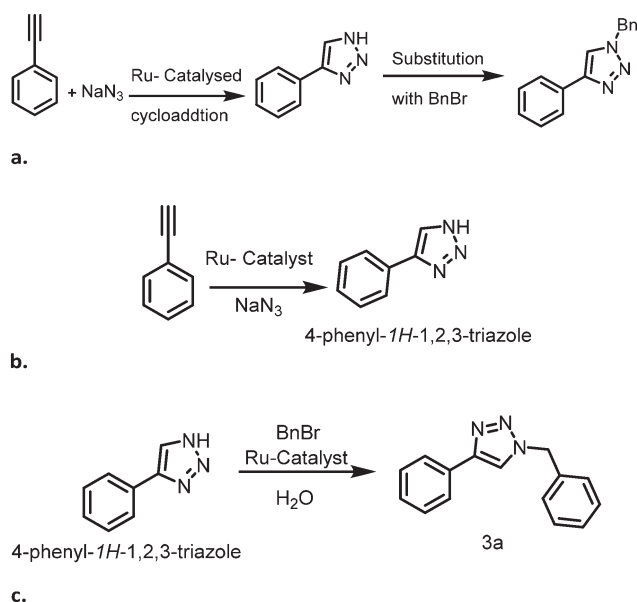
Various carbonyl compounds were hydrogenated under transfer hydrogenation reaction conditions using different alcohols as the hydrogen donor using SBA-15-Tz-Ru(II)TPP catalyst; the results are summarized in Table 6. Carbonyl compounds such as benzaldehyde, cyclohexanone, and acetophenone were hydrogenated smoothly using iso-

propanol to give excellent yields of the corresponding alcohols (Table 6, entries 1–4). Further, aldehydes with electron withdrawing groups, such as 4-chloro and 4-nitro-benzaldehyde, reacted at much faster rates irrespective of the hydrogen donor alcohols (primary, secondary, tertiary) furnishing the corresponding product in excellent yields and with high TON (Table 6, entries 5–10).

To study the heterogeneous nature and stability of the synthesized SBA-15-Tz-Ru(II)TPP catalyst, Sheldon's hot filtration test was carried out, showing that there was nearly no ruthenium leaching into the reaction solution during the course of the reaction. To perform the Sheldon's hot filtration test for the optimized reaction conditions, catalyst SBA-



Scheme 4 Schematic diagram of a model hydrogen transfer reaction using a carbonyl functional (>C=O) group and isopropanol.



Scheme 5 a. Intermediate 4-phenyl-1H-1,2,3-triazole formation. b. Intermediate 4-phenyl-1H-1,2,3-triazole formation via homogeneous catalyst. c. Intermediate 4-phenyl-1H-1,2,3-triazole reacts with BnBr.

**Table 5** Base optimization for catalytic hydrogen transfer reaction

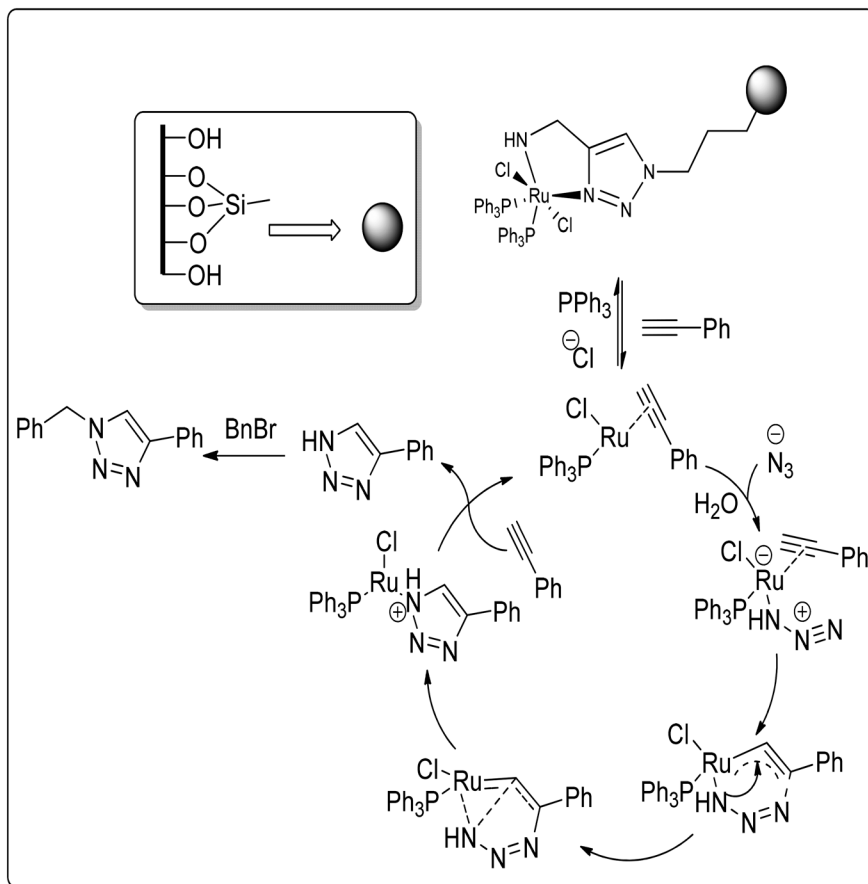
S. No.	Base	Yield (%)
1.	NaOH	100
2.	KOH	98
3.	K <sub>2</sub> CO <sub>3</sub>	50
4.	NaHCO <sub>3</sub>	40
5.	NEt <sub>3</sub>	10

Reaction conditions: SBA-15-Tz-Ru(II)TPP (30 mg, ruthenium metal 0.445 mol%), alcohol (10 mL), carbonyl compound (2 mmol), base (0.5 mmol), 80 °C isolated yields; product analyzed by GC. Conversion based on GC area.

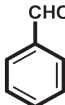

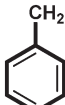
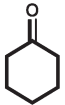
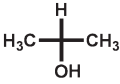
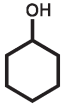
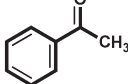
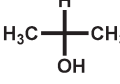
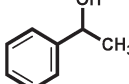
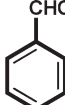
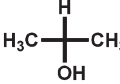
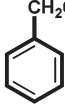
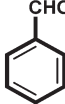
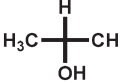
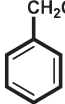
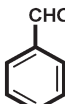
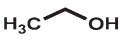
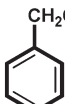
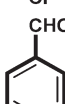

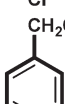
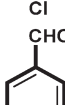
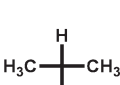
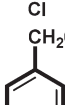
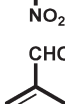

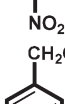
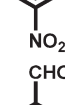

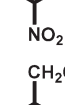
15-Tz-Ru(II)TPP was filtered out from the reaction mixture after 1 h of reaction, and the filtrate was again transferred into the RBF for further continuation of the reaction without catalyst. GC analysis of the filtrate confirmed that the conversion was up to 41% of the corresponding product. As confirmed by GC analysis, there was no improvement in the yield of the hydrogen transferred product, even with prolongation of the hot filtrate reaction by an additional 10 h. Similarly, a hot filtration test of the multicomponent click cycloaddition was also performed under optimized conditions. SBA-15-Tz-Ru(II)TPP catalyst was filtered off from the reaction mixture

after 2 h and the reaction continued uninterrupted in the absence of the heterogeneous catalyst for the next 12 h. GC analysis showed that there was 20% conversion to the corresponding product after 2 h and the further conversion of the multicomponent click cycloaddition remained constant up to 12 h. In both reactions, the results show product formation of more than 80% (ICP result, ESI,† S9).

Further, for the stability and recyclability study of the developed heterogeneous catalyst, SBA-15-Tz-Ru(II)TPP was recycled five times (fresh + four cycles) both in one pot multicomponent click cycloaddition and in the hydrogen transfer reaction. After each cycle, the heterogeneous SBA-15-Tz-Ru(II)TPP catalyst was removed by simple centrifugation, washed several times with a suitable solvent (dichloromethane or ethanol, 10 mL at 80 °C) and dried in an oven overnight (Fig. 11). In every cycle, no considerable change was observed in the conversion and selectivity of the corresponding reaction product. Finally, after the last cycle, the ICP-OES analysis of the used catalyst showed nearly stable ruthenium metal content with respect to the fresh catalyst (ESI,† S9). The conducted experiments confirm the heterogeneous nature of SBA-15-Tz-Ru(II)TPP and its stability, which could be retained after several reaction cycles.

**Fig. 10** Plausible mechanism for the multicomponent click reaction.

**Table 6** Catalytic hydrogen transfer reaction using SBA-15-Tz-Ru(II)TPP catalyst

$\text{R}_1\text{C}(=\text{O})\text{R}_2 + \text{H}_3\text{C}-\text{C}(\text{H})(\text{OH})-\text{CH}_3 \xrightarrow[\text{Base, 80}^\circ\text{C}]{\text{SBA-15-Tz-Ru(II)TPP}} \text{R}_1\text{C}(\text{OH})\text{R}_2 + \text{H}_3\text{C}-\text{C}(=\text{O})-\text{CH}_3$						
Carbonyl group		Alcohol	Alcohol	Carbonyl group		
S. No.	Carbonyl compound	Alcohol	Product	Time (h)	Yield (%)	TON
1.				6	89	200
2.				6	71	160
3.				6	73	164
4.				6	80	180
5.				2	92	207
6.				2	97	218
7.				2	85	191
8.				1	95	213
9.				1.5	99	223
10.				2	80	180

Reaction conditions: SBA-15-Tz-Ru(II)TPP (30 mg, ruthenium metal 0.445 mol%), alcohol (10 mL), carbonyl compound (2 mmol), NaOH (0.5 mmol), 80 °C Isolated yields; product analyzed by GC. Conversion and yield based on GC area.

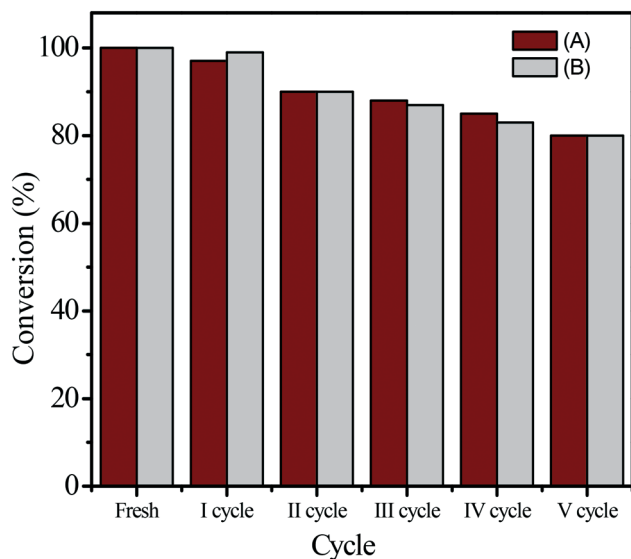


Fig. 11 Recycle study of (A) hydrogen transfer reaction and (B) multicomponent click cycloaddition.

## Conclusions

In summary, we have demonstrated an efficient method for ligand synthesis and covalent tethering to a solid support in a single step using “click chemistry”. A new, highly efficient, heterogeneous SBA-15-Tz-Ru(II)TPP catalyst was developed by immobilizing  $[\text{RuCl}_2(\text{PPh}_3)_3]$  complex over triazole functionalized SBA-15. The catalytic efficiency of SBA-15-Tz-Ru(II)TPP was established for multicomponent click cycloaddition and hydrogen transfer reaction. Surprisingly, the multicomponent cycloaddition reaction exhibited remarkable reactivity in water medium for the regioselective synthesis of 1,4-disubstituted 1,2,3-triazole in excellent yields in contrast to the literature report of 1,5-disubstituted 1,2,3-triazole formation. Additionally, in the hydrogen transfer reactions, the screened carbonyl compounds showed up to 100% conversion to give the hydrogen transferred products. The salient features of the heterogeneous catalyst SBA-15-Tz-Ru(II)TPP are its stability in water as a reaction medium, its heterogeneous nature and recyclability without loss of activity.

### B Synthetic procedures, materials and methods, crystallography

**Experimental.** The materials used, such as Pluronic 123 (P123, average Mol Wt = 5800), tetraethylorthosilicate (TEOS), 3-aminopropyltrimethoxysilane (3-APTMS),  $[\text{RuCl}_2(\text{PPh}_3)_3]$ , sodium azide ( $\text{NaN}_3$ ), *N,N*-diisopropylethylamine (DIPEA), copper iodide (CuI), propargylamine, aldehyde, and alcohols, were purchased from Aldrich. Furthermore, solvents like dichloromethane (DCM), tetrahydrofuran (THF), acetonitrile ( $\text{CH}_3\text{CN}$ ) and toluene were purchased from Merck.

**Synthesis of heterogeneous catalyst SBA-15-Tz-Ru(II)TPP.** The synthesis of SBA-15 was carried out by following the well-established modified literature procedure<sup>27a,28a,29</sup> with the following initial molar compositions: (180.043) TEOS: 4.4 g

$\text{P}_{123}$  Mavg = 5800  $[\text{EO}_{20}\text{-PO}_{70}\text{-EO}_{20}]$ : (8.33)  $\text{H}_2\text{O}$ : (0.24) HCl. Pluronic 123, called  $\text{P}_{123}$  (4.4 g), a triblock co-polymer (surfactant), was dispersed in 30 g of distilled water and stirred for 1.5 h. 120 g of 2 M HCl was added into the solution with constant stirring and continued for a further 2 h. At the same time, 9 g of TEOS (precursor) was added dropwise and the resulting solution was maintained at 35 °C for the next 24 h with stirring. The mixture was kept for hydrothermal treatment at 100 °C for 48 h under static conditions. The obtained material was filtered, washed with distilled water and dried in an oven at 70 °C for 12 h, and later calcined at 540 °C for 8 h in air to get calcined SBA-15 (11.5 g).

**Surface modification over SBA-15 via azide group.** SBA-15 was modified with 3-azidopropyltrimethoxysilane (Az-PTMS) via post grafting method.<sup>8,30a</sup> To 1 g of SBA-15 mixed with 50 mL of toluene, 3.5 mL of 3-azidopropyl trimethoxysilane (Az-PTMS) was added. The resulting mixture was stirred for 12 h at 90 °C in inert atmosphere. After completion of the reaction, the solid was filtered and washed with toluene to remove unreacted 3-Az-PTMS, the further dried at 60 °C for 12 h in an oven to obtain SBA-15- $\text{N}_3$ . Yield: 1.20 g (solid) and preserved under inert atmosphere (Scheme 1B).

**Ligand formation by using SBA-15- $\text{N}_3$  and propargylamine (via click).** Triazole ligand formation over clickable SBA-15 surface was accomplished by following a method described in an earlier report from our group.<sup>8</sup> In a 25 mL round bottom flask with a magnetic stir bar, copper(I) iodide (0.5 mg) and vacuum distilled *N,N*-diisopropylethylamine (DIPEA) (1 mL) were charged with anhydrous, nitrogen-purged dimethylformamide (DMF) (3 mL). The reaction mixture was stirred (till the solution turned green) and, in a further step, transferred to a tetrahydrofuran (THF) reaction mixture (7.5 mL) containing 3-azidopropyltrimethoxysilane (Az-PTMS)-modified mesoporous SBA-15 (SBA-15- $\text{N}_3$ ) (0.5 g). Further, propargylamine (10 mmol) was added and stirred at 50 °C for 12 h. The modified material was ultrasonicated for 20 min, washed with THF, and dried under inert atmosphere. The material was kept in a desiccator in the absence of light for further characterization and modification (Scheme 1C). The obtained material is abbreviated as SBA-15-Tz (yield 0.75 g).

**SBA-15-Tz anchoring by tris(triphenylphosphine)-ruthenium(II) dichloride  $[\text{RuCl}_2(\text{PPh}_3)_3]$  complex.** Modified SBA-15 material (SBA-15-Tz) (1 g) was added to a solution of  $[\text{RuCl}_2(\text{PPh}_3)_3]$  (0.15 mmol) in DMF (50 mL) and refluxed under argon for 12 h. Later, the product was allowed to cool and was then filtered. The obtained gray color solid was washed with THF (25 mL) and acetone (25 mL). Further, the product was Soxhlet extracted with dichloromethane ( $\text{CH}_2\text{Cl}_2$ ) for 24 h to remove unreacted  $[\text{RuCl}_2(\text{PPh}_3)_3]$  and organic impurities (Scheme 1D). The resulting product was dried under vacuum at 75 °C to furnish 1.4 g of the SBA-15-Tz-Ru(II)TPP.

**Multicomponent click reaction.** In a 50 mL round bottom flask, alkyne (1 mmol), sodium azide (1.2 mmol), benzyl bromide (1.2 mmol) and SBA-15-Tz-Ru(II)TPP catalyst (15 mg) were placed, followed by addition of 3 mL of water as the solvent. The mixture was stirred at 90 °C in a preheated oil bath

for the given time. Progress of the reaction was monitored by TLC (2 : 8 ethyl acetate : pet ether). After the completion of the reaction, 10 mL of ethyl acetate was added to the reaction mixture and filtered to recover the SBA-15-Tz-Ru(II)TPP catalyst. The residue was washed with ethyl acetate (5 mL  $\times$  3 times). The combined organic layer was dried with anhydrous sodium sulfate and concentrated under reduced pressure. The crude product was purified by column chromatography to obtain the product 4 a–n (Scheme 3). The product was characterized by GC-MS and  $^1\text{H}$  and  $^{13}\text{C}$  NMR analysis (ESI,† S10 and S11).

**Hydrogen transfer reaction.** In a 25 mL two-neck round-bottom flask, carbonyl compounds (2 mmol), NaOH (0.5 mmol), alcohol (isopropanol) (10 mL), and SBA-15-Tz-Ru(II)TPP catalyst (30 mg) were stirred under argon at 80 °C. The reaction mixture was analyzed by GC at measured time intervals (Scheme 4).

## Results and discussion

**Characterization.** Powder X-ray diffraction (XRD) patterns were measured on a PAN analytical X'pert Pro dual goniometer diffractometer using Ni-filtered  $\text{CuK}\alpha$  radiation ( $l = 1.5404 \text{ \AA}$ ) over the range 0.5–51 (SAXRD).  $\text{N}_2$  adsorption–desorption isotherms, pore size distributions as well as the textural properties of the hybrid materials were determined by using an Autosorb 1C (Quantachrome, USA). The program, consisting of both an adsorption and desorption branch, typically ran at  $-196 \text{ }^\circ\text{C}$  after samples were degassed at  $150 \text{ }^\circ\text{C}$  for 4 h. The BET method was applied to calculate the total surface area at relative pressures of  $P/P_0 = 0.65\text{--}0.45$  and the BJH model was applied to the adsorption branch of the isotherm to determine the total pore volume and average pore diameter at a relative pressure of  $P/P_0 = 0.99$ . Pore size distribution curves were obtained *via* the NLDFT model, assuming cylindrical pore geometry. Magic angle spinning (MAS) NMR spectra of  $^{29}\text{Si}$ ,  $^{31}\text{P}$  and  $^{13}\text{C}$  nuclei were recorded on a Bruker DSX300 spectrometer at 7.05 T (resonance frequencies: 59.595 MHz and 75.43 MHz, rotor speed 10 000 Hz and 10 000 Hz). XPS analysis was conducted using an XPS Kratos AXIS Ultra (Kratos Analytical Ltd., UK) high-resolution photoelectron spectroscopy instrument. FTIR spectra were recorded on a Bruker Alpha-T. Sample morphology was observed by extra high-resolution scanning electron microscopy (Magellan™ 400 L). Thermal analysis (TGA) of the samples was conducted using a Pyris Diamond TGA analyzer with a heating rate of  $100 \text{ }^\circ\text{C min}^{-1}$  under air atmosphere. GC analyses were performed using a Focus GC from Thermo Electron Corporation, equipped with a low polarity ZB-5 column or using a Trace 1300 gas chromatograph from Thermo Scientific, equipped with an Rxi-1 ms (crossbond 100% dimethyl polysiloxane) column. Conversion was based on GC area. The ruthenium (Ru) content of the product was determined by an inductively coupled plasma mass spectrometry (ICPMS) (Agilent 7500 cx).

## Conflicts of interest

There are no conflicts to declare.

## Acknowledgements

APS acknowledges CSIR, New Delhi for the financial support in the form of an Emeritus Scientist project (P81103). PK is grateful to INSA, New Delhi for financial support under the senior scientist program. Jayant Rathod thanks the Council of Scientific and Industrial Research (CSIR), New Delhi for a Senior Research Fellowship. P. Sharma gratefully acknowledges Grant No. ISF 207/12 (Israel grant) for financial support.

## Notes and references

- (a) H. C. Kolb and K. B. Sharpless, *Drug Discovery Today*, 2003, **8**, 1128–1137; (b) D. Dheer, V. Singh and R. Shankar, *Bioorg. Chem.*, 2017, **71**, 30–54.
- J.-F. Lutz and Z. Zarafshani, *Adv. Drug Delivery Rev.*, 2008, **60**, 958–970.
- (a) R. Huisgen, G. Szeimies and L. Möbius, *Chem. Ber.*, 1967, **100**, 2494–2507; (b) M. S. Singh, S. Chowdhury and S. Koley, *Tetrahedron*, 2016, **72**, 5257–5283.
- (a) H. Struthers, T. L. Mindt and R. Schibli, *Dalton Trans.*, 2010, **39**, 675–696; (b) T. Romero, R. A. Orenes, A. Espinosa, A. Tárraga and P. Molina, *Inorg. Chem.*, 2011, **50**, 8214–8224; (c) J. P. Byrne, J. A. Kitchen and T. Gunnlaugsson, *Chem. Soc. Rev.*, 2014, **43**, 5302–5325.
- R. M. Meudtner, M. Ostermeier, R. Goddard, C. Limberg and S. Hecht, *Chem. – Eur. J.*, 2007, **13**, 9834–9840.
- (a) D. Schweinfurth, R. Pattacini, S. Strobel and B. Sarkar, *Dalton Trans.*, 2009, 9291–9297; (b) D. Schweinfurth, C.-Y. Su, S.-C. Wei, P. Braunstein and B. Sarkar, *Dalton Trans.*, 2012, **41**, 12984–12990.
- J. D. Crowley and D. A. McMorran, in *Click Triazoles*, ed. J. Košmrlj, Springer Berlin Heidelberg, Berlin, Heidelberg, 2012, pp. 31–83.
- P. Sharma and A. P. Singh, *RSC Adv.*, 2014, **4**, 43070–43079.
- S.-H. Cho, T. Gadzikwa, M. Afshari, S. T. Nguyen and J. T. Hupp, *Eur. J. Inorg. Chem.*, 2007, **2007**, 4863–4867.
- (a) C. T. Kresge, M. E. Leonowicz, W. J. Roth, J. C. Vartuli and J. S. Beck, *Nature*, 1992, **359**, 710–712; (b) J. S. Beck, J. C. Vartuli, W. J. Roth, M. E. Leonowicz, C. T. Kresge, K. D. Schmitt, C. T. W. Chu, D. H. Olson, E. W. Sheppard, S. B. McCullen, J. B. Higgins and J. L. Schlenker, *J. Am. Chem. Soc.*, 1992, **114**, 10834–10843.
- (a) R. D. Patil and Y. Sasson, *Asian J. Org. Chem.*, 2015, **4**, 1258–1261; (b) S.-Q. Bai, L. Jiang, J.-L. Zuo and T. S. A. Hor, *Dalton Trans.*, 2013, **42**, 11319–11326; (c) Z. Gonda and Z. Novak, *Dalton Trans.*, 2010, **39**, 726–729; (d) D. Wang, M. Zhao, X. Liu, Y. Chen, N. Li and B. Chen, *Org. Biomol. Chem.*, 2012, **10**, 229–231; (e) F. Wang, H. Fu, Y. Jiang and Y. Zhao, *Green Chem.*, 2008, **10**, 452–456.
- (a) L. Jiang, Z. Wang, S.-Q. Bai and T. S. A. Hor, *Dalton Trans.*, 2013, **42**, 9437–9443; (b) F. Nador, M. A. Volpe, F. Alonso, A. Feldhoff, A. Kirschning and G. Radivoy, *Appl. Catal., A*, 2013, **455**, 39–45.
- (a) M. Singla, P. Mathur, M. Gupta and M. S. Hundal, *Transition Met. Chem.*, 2008, **33**, 175–182; (b) K. R.

- Gruenwald, A. M. Kirillov, M. Haukka, J. Sanchiz and A. J. L. Pombeiro, *Dalton Trans.*, 2009, 2109–2120.
- 14 (a) C. Wang, D. Ikhlef, S. Kahlal, J.-Y. Saillard and D. Astruc, *Coord. Chem. Rev.*, 2016, 316, 1–20; (b) A. Tăbăcaru, B. Furdui, I. O. Ghinea, G. Cârăc and R. M. Dinică, *Inorg. Chim. Acta*, 2017, 455, 329–349.
- 15 J. R. Johansson, T. Beke-Somfai, A. Said Stålsmeden and N. Kann, *Chem. Rev.*, 2016, 116, 14726–14768.
- 16 (a) B. C. Boren, S. Narayan, L. K. Rasmussen, L. Zhang, H. Zhao, Z. Lin, G. Jia and V. V. Fokin, *J. Am. Chem. Soc.*, 2008, 130, 8923–8930; (b) S. Oppiliart, G. Mousseau, L. Zhang, G. Jia, P. Thuéry, B. Rousseau and J.-C. Cintrat, *Tetrahedron*, 2007, 63, 8094–8098; (c) M. M. Majireck and S. M. Weinreb, *J. Org. Chem.*, 2006, 71, 8680–8683; (d) Y.-H. Lo, T.-H. Wang, C.-Y. Lee and Y.-H. Feng, *Organometallics*, 2012, 31, 6887–6899; (e) D.-R. Hou, T.-C. Kuan, Y.-K. Li, R. Lee and K.-W. Huang, *Tetrahedron*, 2010, 66, 9415–9420.
- 17 P. N. Liu, J. Li, F. H. Su, K. D. Ju, L. Zhang, C. Shi, H. H. Y. Sung, I. D. Williams, V. V. Fokin, Z. Lin and G. Jia, *Organometallics*, 2012, 31, 4904–4915.
- 18 (a) J.-E. Bäckvall, *J. Organomet. Chem.*, 2002, 652, 105–111; (b) X. Wu and J. Xiao, *Chem. Commun.*, 2007, 2449–2466; (c) S. E. Clapham, A. Hadzovic and R. H. Morris, *Coord. Chem. Rev.*, 2004, 248, 2201–2237; (d) P. Albin, J. Blum, E. Dunkelblum and Y. Sasson, *J. Org. Chem.*, 1975, 40, 2402–2403.
- 19 (a) G. Brieger and T. J. Nestrick, *Chem. Rev.*, 1974, 74, 567–580; (b) R. A. W. Johnstone, A. H. Wilby and I. D. Entwistle, *Chem. Rev.*, 1985, 85, 129–170; (c) P. K. Mandal and J. S. McMurray, *J. Org. Chem.*, 2007, 72, 6599–6601.
- 20 R. Tao, Y. Xie, G. An, K. Ding, H. Zhang, Z. Sun and Z. Liu, *J. Colloid Interface Sci.*, 2010, 351, 501–506.
- 21 S. U. Sonavane and R. V. Jayaram, *Synth. Commun.*, 2003, 33, 843–849.
- 22 L. He, J. Ni, L.-C. Wang, F.-J. Yu, Y. Cao, H.-Y. He and K.-N. Fan, *Chem. – Eur. J.*, 2009, 15, 11833–11836.
- 23 (a) X. Wu, J. Liu, X. Li, A. Zanotti-Gerosa, F. Hancock, D. Vinci, J. Ruan and J. Xiao, *Angew. Chem., Int. Ed.*, 2006, 45, 6718–6722; (b) A. Bényei and F. Joó, *J. Mol. Catal. A: Chem.*, 1990, 58, 151–163.
- 24 (a) T. Ikariya and A. J. Blacker, *Acc. Chem. Res.*, 2007, 40, 1300–1308; (b) F.-Z. Su, L. He, J. Ni, Y. Cao, H.-Y. He and K.-N. Fan, *Chem. Commun.*, 2008, 3531–3533.
- 25 (a) W. Ye, M. Zhao, W. Du, Q. Jiang, K. Wu, P. Wu and Z. Yu, *Chem. – Eur. J.*, 2011, 17, 4737–4741; (b) J. Toubiana and Y. Sasson, *Catal. Sci. Technol.*, 2012, 2, 1644–1653.
- 26 (a) W. Ye, M. Zhao and Z. Yu, *Chem. – Eur. J.*, 2012, 18, 10843–10846; (b) S. Gladioli and E. Alberico, *Chem. Soc. Rev.*, 2006, 35, 226–236.
- 27 (a) P. Sharma and A. P. Singh, *RSC Adv.*, 2014, 4, 58467–58475; (b) A. Lazar, W. R. Thiel and A. P. Singh, *RSC Adv.*, 2014, 4, 14063–14073.
- 28 (a) A. Lazar, C. P. Vinod and A. P. Singh, *New J. Chem.*, 2016, 40, 2423–2432; (b) D. Zhao, J. Feng, Q. Huo, N. Melosh, G. H. Fredrickson, B. F. Chmelka and G. D. Stucky, *Science*, 1998, 279, 548–552.
- 29 A. Lazar, P. Sharma and A. P. Singh, *Microporous Mesoporous Mater.*, 2013, 170, 331–339.
- 30 (a) M. Kar, B. Malvi, A. Das, S. Panneri and S. S. Gupta, *J. Mater. Chem.*, 2011, 21, 6690–6697; (b) B. Malvi, B. R. Sarkar, D. Pati, R. Mathew, T. G. Ajithkumar and S. Sen Gupta, *J. Mater. Chem.*, 2009, 19, 1409–1416; (c) J. Gao, X. Zhang, S. Xu, J. Liu, F. Tan, X. Li, Z. Qu, Y. Zhang and X. Quan, *Chem. – Asian J.*, 2014, 9, 908–914.
- 31 (a) A. Ghosh and R. Kumar, *Microporous Mesoporous Mater.*, 2005, 87, 33–44; (b) T. Joseph, S. S. Deshpande, S. B. Halligudi, A. Vinu, S. Ernst and M. Hartmann, *J. Mol. Catal. A: Chem.*, 2003, 206, 13–21.
- 32 S. Sisodiya, A. Lazar, S. Shylesh, L. Wang, W. R. Thiel and A. P. Singh, *Chem. Commun.*, 2012, 25, 22–27.
- 33 S. Farsadpour, L. T. Ghoochany, S. Shylesh, G. Dörr, A. Seifert, S. Ernst and W. R. Thiel, *ChemCatChem*, 2012, 4, 401–407.
- 34 (a) A. Jana, J. Mondal, P. Borah, S. Mondal, A. Bhaumik and Y. Zhao, *Chem. Commun.*, 2015, 51, 10746–10749; (b) C. Agnes, J.-C. Arnault, F. Omnes, B. Jousset, M. Billon, G. Bidan and P. Mailley, *Phys. Chem. Chem. Phys.*, 2009, 11, 11647–11654.
- 35 (a) B. Dervaux and F. E. Du Prez, *Chem. Sci.*, 2012, 3, 959–966; (b) V. Bénétou, A. Olmos, T. Boningari, J. Sommer and P. Pale, *Tetrahedron Lett.*, 2010, 51, 3673–3677; (c) E. Ozkal, S. Ozcubukcu, C. Jimeno and M. A. Pericas, *Catal. Sci. Technol.*, 2012, 2, 195–200.
- 36 (a) B. H. Lipshutz and B. R. Taft, *Angew. Chem.*, 2006, 118, 8415–8418; (b) M. Nasr-Esfahani, I. Mohammadpoor-Baltork, A. R. Khosropour, M. Moghadam, V. Mirkhani, S. Tangestaninejad and H. Amiri Rudbari, *J. Org. Chem.*, 2014, 79, 1437–1443.
- 37 (a) H. Sharghi, M. H. Beyzavi, A. Safavi, M. M. Doroodmand and R. Khalifeh, *Adv. Synth. Catal.*, 2009, 351, 2391–2410; (b) H. Sharghi, R. Khalifeh and M. M. Doroodmand, *Adv. Synth. Catal.*, 2009, 351, 207–218.
- 38 B. C. Boren, S. Narayan, L. K. Rasmussen, L. Zhang, H. Zhao, Z. Lin, G. Jia and V. V. Fokin, *J. Am. Chem. Soc.*, 2008, 130, 8923–8930.
- 39 (a) A. Aranyos, G. Csajnyik, K. J. Szabo and J.-E. Backvall, *Chem. Commun.*, 1999, 351–352; (b) R. L. Chowdhury and J.-E. Backvall, *J. Chem. Soc., Chem. Commun.*, 1991, 1063–1064; (c) S. Mazza, R. Scopelliti and X. Hu, *Organometallics*, 2015, 34, 1538–1545.
- 40 (a) G. Z. Wang and J.-E. Backvall, *J. Chem. Soc., Chem. Commun.*, 1992, 337–339; (b) Y. R. S. Laxmi and J.-E. Backvall, *Chem. Commun.*, 2000, 611–612.
- 41 (a) R. Langer, G. Leitius, Y. Ben-David and D. Milstein, *Angew. Chem., Int. Ed.*, 2011, 50, 2120–2124; (b) A. Mikhailine, A. J. Lough and R. H. Morris, *J. Am. Chem. Soc.*, 2009, 131, 1394–1395.